Nano Energy 52 (2018) 416–421

Contents lists available at ScienceDirect

Nano Energy

journal homepage: www.elsevier.com/locate/nanoen

Full paper

Adjustment and control on the fundamental characteristics of a piezoelectric PN junction by mechanical-loading

Shuaiqi Fan, Wanli Yang, Yuantai Hu*

Department of Mechanics, Hubei Key Laboratory of Engineering Structural Analysis and Safety Assessment, Huazhong University of Science and Technology, Wuhan 430074, China

ARTICLE INFO

Keywords:
PN junction
Piezoelectric property
Depletion layer
Contact potential difference
Potential barrier

ABSTRACT

The nonlinear governing equations on the electromechanical coupling and carrier concentrations are established for a static piezoelectric PN junction subjected to a pair of tensile/compressive stresses at the endpoints. Numerical results show adjustability and controllability on the fundamental characteristics of a piezoelectric PN junction by mechanical-loading. A pair of tensile-stresses induces enlargement of both depletion layer width and contact potential difference of a piezoelectric PN junction, where the majority carrier concentration is increased and the minority one is decreased. Thus, potential barrier of the PN junction is raised by tensile-stressed loading such that it becomes more difficult to break-through. Correspondingly, a pair of compressive-stresses results in diminishing of depletion layer width and contact potential difference of a piezoelectric PN junction, where the majority carrier concentration is decreased and the minority one is increased. Thus, potential barrier of the PN junction is reduced by compressive-stressed loading such that it becomes easier to break-through. Moreover, analysis indicates that a shorter distance between the loading point and the depletion layer is able to produce better adjustment and control effect. This technique by coupled electromechanical fields and carrier concentrations as a whole has some referential significance to piezotronics.

1. Introduction

When a semiconductor is with piezo-effect, loading induced deformations stir up polarization electric fields due to electromechanical coupling, and the polarization electric fields drive charge carriers into redistributions/motion. Conversely, carrier redistribution/motion produces screening effect on polarization electric fields per se, and further exerts influence on deformations [1–3]. Such interaction between electromechanical quantities and charge carriers can be used to develop many new microelectronic devices with modern functions, for example energy harvesters for converting mechanical energy into electrical energy [4–10], field effect transistors [11–18], acoust charge transport devices [19], as well as strain, gas, humidity and chemical sensors [20,21], etc. PN junction is an important core component in the development of many semiconductor devices [22–25], understanding the nature of PN junctions is the basis for analyzing the characteristics of these devices. PN junction consists of two semiconductors with different type doping in general. As well known, electrons are majority carriers and holes are minority ones in an n-type semiconductor, while the opposite is happening in a p-type semiconductor. When these two kinds of semiconductors are contacted together to form a PN junction, gradients of electron and hole concentrations appear near the interface, which certainly drive the holes to diffuse from the p-zone to the n-zone and the electrons from the n-zone to the p-zone. According to the hypothesis of depletion layer, carrier diffusions induce appearance of a space charge zone (SCZ) near the interface, consisting of a donor layer in the n-type region and an acceptor layer in the p-type region. It should be noted that doping can usually be considered as completely ionized at room temperature [26]. Both the depletion layer width and the contact potential difference are two important parameters to embody the fundamental characteristics of a PN junction, which are influenced by carrier concentrations and material property. When the two semiconductors to constitute a PN junction are with piezo-effect, the fundamental characteristics of the PN junction, for example depletion layer width, contact potential difference and carrier concentrations, can be adjusted and controlled by mechanical- loading. Thus, some researchers have paid attention on this topic. Zhang et al. extended the depletion layer hypothesis into piezoelectric PN junction by introducing a polarization charge layer at the interface in the space charge zone [16,27]. A lot of interesting results have been obtained qualitatively, although the resultant solution depends on the width of polarization charge layer w_{piezo} which keeps undetermined. Luo et al. analyzed a circular

* Corresponding author.
E-mail address: hudeng@263.net (Y. Hu).

https://doi.org/10.1016/j.nanoen.2018.08.017
Received 2 July 2018; Received in revised form 1 August 2018; Accepted 8 August 2018
Available online 09 August 2018
2211-2855/

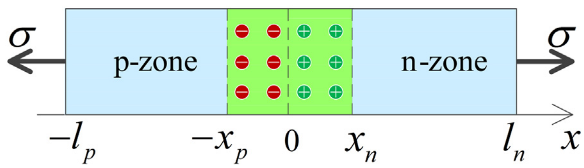

Fig. 1. A piezoelectric PN junction subjected to a pair of tensile-stresses.

piezoelectric PN junction subjected to anti-plane deformations [25], where an assumption of linear fluctuation of carrier concentration has been applied.

This paper is concerned with the exact solutions in a piezoelectric PN junction subjected to a pair of tensile/compressive stresses by the theory of multi-field coupling. The nonlinear governing equations of electromechanical coupling and carrier concentrations are established in Section 2 together with giving the conditions of determining solutions. A lot of numerical results and discussions for a piezoelectric PN junction subjected to a pair of tensile or compressive stresses are quantitatively conducted in Section 3. It is found that mechanical-loading of tensile/compressive stresses induces increase/decrease of potential barrier of a piezoelectric PN junction and makes it to become more difficult/easier to break-through. This ensures the adjustability and controllability of performance of a piezoelectric PN junction. Finally some useful conclusions have been drawn in Section 4.

2. Analysis on a static piezoelectric PN junction

Fig. 1 schematically shows a piezoelectric PN junction subjected to a pair of tensile/compressive stresses σ at the two endpoints, formed by a p-type and a n-type ZnO rod contacted at $x = 0$. Both ZnO rods are with the c-axis in the x-direction. The n-zone is with electrons as majority carriers and holes as minority carriers, the p-zone is just with the opposite. In the depleted layer $-x_p < x < 0$, holes have been depleted where the acceptor ions with negative charges are left, and in the depleted layer $0 < x < x_n$, electrons have been depleted where the donor ions with positive charges are left.

The one-dimensional Gauss law can be written as [28,29]

$$\frac{\mathrm{d}D}{\mathrm{d}x} = \begin{cases} q(\Delta p_p(x) - \Delta n_p(x)), & -l_p < x < -x_p, \\ -qN_A, & -x_p < x < 0, \\ qN_D, & 0 < x < x_n, \\ q(\Delta p_n(x) - \Delta n_n(x)), & x_n < x < l_n, \end{cases} \tag{1}$$

where p and n stand for hole and electron concentrations, respectively; N_A and N_D are acceptor and donor concentrations, respectively. D denotes electric displacement; q(=1.6 × 10^{-19}C) is electron charge. When a pair of tension/compressive stresses σ is applied at the two endpoints of the piezoelectric PN junction, D can be obtained as

$$D = (e_{33}/c_{33})\sigma + \bar{\varepsilon}_{33}E, \tag{2}$$

where $\sigma = c_{33}S - e_{33}E$, $D = e_{33}S + \varepsilon_{33}E$, $\bar{\varepsilon}_{33} = (1 + k_{33}^2)\varepsilon_{33}$ and $k_{33}^2 = e_{33}^2/(c_{33}\varepsilon_{33})$. In the above, $S = du/\mathrm{d}x$ and $E = -\mathrm{d}\phi/\mathrm{d}x$ stand for strain and electric field, respectively; u and ϕ are displacement and electric potential, respectively; c_{33}, e_{33} and ε_{33} are elastic, piezoelectric, and dielectric constants. The null current conditions require $(J_p, J_n) = q(p\mu_{p33}E - \kappa_{p33}\mathrm{d}p/\mathrm{d}x,\quad n\mu_{n33}E + \kappa_{n33}\mathrm{d}n/\mathrm{d}x) = (0, 0)$, which yield

$$\begin{pmatrix} p_p \\ n_p \end{pmatrix}(x) = \begin{pmatrix} p_p & (-x_p) \\ n_p & (-x_p) \end{pmatrix}\exp\left[\begin{pmatrix} - \\ + \end{pmatrix}\frac{q}{kT}(\phi(x) - \phi(-x_p))\right],$$
for $\quad -l_p < x < -x_p$,
$$\begin{pmatrix} p_n \\ n_n \end{pmatrix}(x) = \begin{pmatrix} p_n & (x_n) \\ n_n & (x_n) \end{pmatrix}\exp\left[\begin{pmatrix} - \\ + \end{pmatrix}\frac{q}{kT}(\phi(x) - \phi(x_n))\right],$$
for $\quad x_n < x < l_n$. (3)

In the above, $(\mu_{p33}, \kappa_{p33})$ and $(\mu_{n33}, \kappa_{n33})$ are mobility and diffusion coefficients of holes and electrons, respectively. Subscripts "p" and "n" stand for p-zone and n-zone, respectively. k (=8.62 × 10^{-16}erg/$^{\mathrm{o}}$C) is the Boltzmann constant and T represents the temperature which has been chosen as 300 K in our analysis. The relationship, $\mu_{p33}/\kappa_{p33} = \mu_{n33}/\kappa_{n33} = q/kT$, has been used in deriving (3). Obviously, for a static piezoelectric PN junction subjected to zero stress, $\sigma = 0$, the electric potential in the n-zone can be determined as V_D^0 when the electric potential of the p-zone is chosen as null according to the semiconductor theory [26]. V_D^0 stands for the initial contact potential difference of the space charge zone and can be determined by the doped concentrations in both the p-zone and the n-zone as

$$V_D^0 = 2.3(kT/q)\log(N_D N_A/n_i^2), \tag{4}$$

where n_i stands for the intrinsic carrier concentration of ZnO. Initial carrier concentrations at $\sigma = 0$ are denoted as p_{p0} and n_{p0} in the p-zone, and as p_{n0} and n_{n0} in the n-zone, respectively, which satisfy

$$(p_{n0}, n_{p0}) = (p_{p0}, n_{n0})\exp(-qV_D^0/kT). \tag{5}$$

When σ becomes non-zero, the loading induced deformation stimulates polarization electric field due to the piezo-effect. The polarization electric field drives carrier redistribution, and thus, electric potential in the whole PN junction region shown in Fig. 1 should become different. Obviously, such change of potential field is related to carrier concentrations. It follows from [27] that

$$\begin{pmatrix} p_p \\ n_p \end{pmatrix}(-x_p) = \begin{pmatrix} p_{p0} \\ n_{p0} \end{pmatrix}\exp\left(\begin{pmatrix} - \\ + \end{pmatrix}q\phi(-x_p)/kT\right),$$
$$\begin{pmatrix} p_n \\ n_n \end{pmatrix}(x_n) = \begin{pmatrix} p_{n0} \\ n_{n0} \end{pmatrix}\exp\left(\begin{pmatrix} - \\ + \end{pmatrix}q(\phi(x_n) - V_D^0)/kT\right). \tag{6}$$

Substituting (6) into (3), we have

$$\begin{pmatrix} p_p \\ n_p \end{pmatrix}(x) = \begin{pmatrix} p_{p0} \\ n_{p0} \end{pmatrix}\exp\left[\begin{pmatrix} - \\ + \end{pmatrix}\frac{q}{kT}\phi(x)\right], \qquad \text{for} \quad -l_p < x < -x_p,$$
$$\begin{pmatrix} p_n \\ n_n \end{pmatrix}(x) = \begin{pmatrix} p_{n0} \\ n_{n0} \end{pmatrix}\exp\left[\begin{pmatrix} - \\ + \end{pmatrix}\frac{q}{kT}(\phi(x) - V_D^0)\right], \qquad \text{for} \quad x_n < x < l_n. \tag{7}$$

Thus, we get

$$\begin{pmatrix} \Delta p_p & (x) \\ \Delta n_p & (x) \end{pmatrix} = \begin{pmatrix} p_{p0} \\ n_{p0} \end{pmatrix}\left[\exp\left(\begin{pmatrix} - \\ + \end{pmatrix}\frac{q}{kT}\phi(x)\right) - 1\right],$$
for $\quad -l_p < x < -x_p$,
$$\begin{pmatrix} \Delta p_n & (x) \\ \Delta n_n & (x) \end{pmatrix} = \begin{pmatrix} p_{n0} \\ n_{n0} \end{pmatrix}\left[\exp\left(\begin{pmatrix} - \\ + \end{pmatrix}\frac{q}{kT}(\phi(x) - V_D^0)\right) - 1\right],$$
for $\quad x_n < x < l_n$. (8)

Use of the depletion layer hypothesis and the charge balance condition yields

$$N_A x_p = N_D x_n. \tag{9}$$

Solving the potential field in $-x_p < x < x_n$, we obtain the present contact potential difference V_D of SCZ under nonzero σ,

$$V_D = \phi(x_n) - \phi(-x_p) = (q/2\bar{\varepsilon}_{33})(N_A x_p^2 + 2N_A x_p x_n - N_D x_n^2). \tag{10}$$

For a static piezoelectric PN junction under a thermal equilibrium state, we assume the conditions of determining electromechanical solutions as follows:

1) Null electric displacement at the two endpoints $x = -l_p$ and $x = l_n$;
2) Continuity for electric potential and electric displacement at $x = 0$, $-x_p$ and x_n, respectively;
3) The boundaries of SCZ require $E(-x_p) = E(x_n) = 0$.

Substituting (2) and (8) into (1), a second-order differential equation for electric potential field ϕ in the whole PN junction region can be established. By applied the determining-solution conditions together with (9) and (10), electric potential field ϕ in the whole PN junction region can be achieved. In this paper, the initial boundaries of SCZ at $\sigma = 0$ are designed as x_p^0 and x_n^0.

3. Numerical results and discussions

We calculate the electric potential field, carrier concentrations in a static piezoelectric PN junction after subjected to a pair of tensile/compressive stresses σ. The material constants of a ZnO rod with the c-axis in the x-direction are as follows [30–32] with $\varepsilon_0 = 8.8542 \times 10^{-12}$ F/ m:

$$c_{33} = 209.5\text{GPa}, \quad e_{33} = 1.22\text{C/m}^2, \quad \varepsilon_{33} = 11.9\varepsilon_0 . \tag{11}$$

Take the initial doping concentrations of the p-type and the n-type ZnO rods as

$$p_{p0} = n_{n0} = 1 \times 10^{20}(\text{m}^{-3}), \tag{12}$$

with $n_{p0}p_{p0} = n_{n0}p_{n0} = n_i^2$, $n_i = 1 \times 10^{16}(\text{m}^{-3})$. The initial lengths of p-type zone and n-type zone are taken as $l_p - x_p^0 = l_n - x_n^0$. $x_p^0 = x_n^0$ is due to the same doping concentrations in (12). Because $N_A \cong p_{p0}$ and $N_D \cong n_{n0}$, it is readily obtained from (4) that the initial contact potential difference of SCZ $V_D^0 = 0.4758$V and the initial SCZ size $X_D^0 = x_p^0 + x_n^0 = 3.6570\mu$m from $X_D^0 = \sqrt{2\bar{\varepsilon}_{33}V_D^0(N_A + N_D)/(qN_AN_D)}$.

First, we discuss a piezoelectric PN junction subjected to a pair of tensile-stresses. Fig. 2 explicitly shows dependence of $\overline{V}_D = V_D/V_D^0$ and $\overline{X}_D = X_D/X_D^0$ upon the non-dimensional tensile-stress $\overline{\sigma} = \sigma/\sigma_0$ ($\sigma_0 = 1$MPa) for different $l_p/x_p^0(l_n/x_n^0)$. In the initial stage, both quantities monotonously increase with enlargement of $\overline{\sigma}$ for a fixed $l_p/x_p^0(l_n/x_n^0)$, and then, approach two certain definite values. Moreover, the larger $l_p/x_p^0(l_n/x_n^0)$ is corresponding to the smaller $\overline{V}_D$ and $\overline{X}_D$.

As well known, deformations of a piezoelectric semiconductor stir up polarization electric fields to drive carriers into redistribution, and carrier redistribution produces weakening influence on polarization electric fields per se. That carrier concentrations are uniform in both the end regions of a piezoelectric PN junction at $\overline{\sigma} = 0$ implies a small weakening influence at the initial stage from carrier redistribution induced electric field (CRIEF) to deformation induced polarization electric field (DIPEF). As $\overline{\sigma}$ increases, the weakening effect gradually becomes enhanced to result in reduction in the variant rates of $\overline{V}_D$ and $\overline{X}_D$. Finally, both the size and the contact potential difference of SCZ tend to two definite values once the augmentation effect produced by mechanical-loading is just counteracted by the reduction effect caused by carrier redistribution. In addition, we also read from Fig. 2 that for a fixed x_p^0, a smaller l_p/x_p^0 produces larger $\overline{V}_D$ and $\overline{X}_D$. The reason can be illustrated as follows: a larger distance $l_p - x_p^0$ between the loading point and SCZ, a longer action region (AR) for CRIEF to produce weakening effect on DIPEF, and thus, a smaller influence from external mechanical-loading on SCZ; Conversely, a smaller $l_p - x_p^0$ is corresponding to a shorter AR for CRIEF to produce weakening on DIPEF, and thus, a bigger influence from external mechanical-loading to SCZ. Fig. 3 shows distribution of electric potential field in a piezoelectric PN junction where $\overline{x} = x/x_p^0$. In [33], all the electric field in a tensile-stressed ZnO rod with c-axis in the positive x-direction has been verified to be negative. The corresponding electric potential has also been shown to be negative in the left portion and positive in the right one. Based on the results in [33], it is easy to deduce that for a tensile-stressed piezoelectric PN junction shown in Fig. 1, the electric potential increment in the p-zone should be negative and in the n-zone should be positive. In addition, we also note from Fig. 3 that the interaction between the end loading at $\overline{x} = -l_p/x_p^0$ and SCZ is very weak for $l_p/x_p^0 = 2.0$. This is because AR is relatively too long under $l_p/x_p^0 = 2.0$ such that CRIEF has enough distance to weaken DIPEF. As l_p/x_p^0 gradually becomes small, large electric potential increment will be aroused near SCZ boundaries, as shown in Fig. 3 for $l_p/x_p^0 = 1.5$ and 1.3, which will certainly stir up apparent carrier redistribution at $\overline{x} = \pm 1$.

Following, we discuss the carrier redistribution characteristics in a tensile-stressed piezoelectric PN junction due to mechanical-loading. Fig. 4 shows the carrier concentrations for three different configurations: $l_p/x_p^0 = 1.3, 1.5, 2.0$, respectively, under $x_p^0 = 1.8285\mu$m. It should be noted that in obtaining distribution of carrier concentrations, we have used the following expressions to get the carrier concentrations in SCZ $-x_p < x < x_n$ [26]:

$$p(x) = p_p(-x_p)\exp\left[\frac{q}{kT}(\phi(-x_p) - \phi(x))\right],$$
$$n(x) = n_n(x_n)\exp\left[-\frac{q}{kT}(\phi(x_n) - \phi(x))\right]. \tag{13}$$

In addition, all carrier concentrations in Fig. 4 have been dimensionless as follows

$$(\overline{p}(x), \overline{n}(x)) = \begin{cases} \log(p_p(x)/p_{p0}, n_p(x)/n_{n0}), & -l_p < x < -x_p, \\ \log(p(x)/p_{p0}, n(x)/n_{n0}), & -x_p < x < x_n, \\ \log(p_n(x)/p_{p0}, n_n(x)/n_{n0}), & x_n < x < l_n. \end{cases} \tag{14}$$

It follows from Fig. 3 that the electric potential increment in the p-type zone ($-l_p < x < -x_p$) is $\phi(x) < 0$ and the electric potential increment in the n-type zone ($x_n < x < l_n$) is $\phi(x) - V_D^0 > 0$. Thus, every electron in the p-type zone obtains an electric potential energy change $-q\phi(x)$ and in the n-type one obtains an electric potential energy change $-q[\phi(x) - V_D^0]$. Then, the intrinsic energy level of electrons

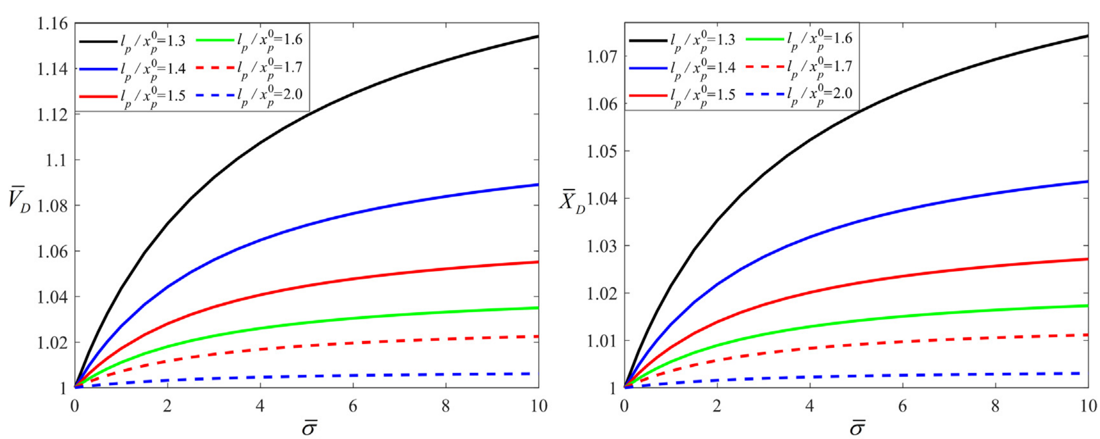

Fig. 2. Dependence of both the contact potential difference and the size of SCZ in a piezoelectric PN junction subjected to a pair of tensile-stresses for different l_p/x_p^0.

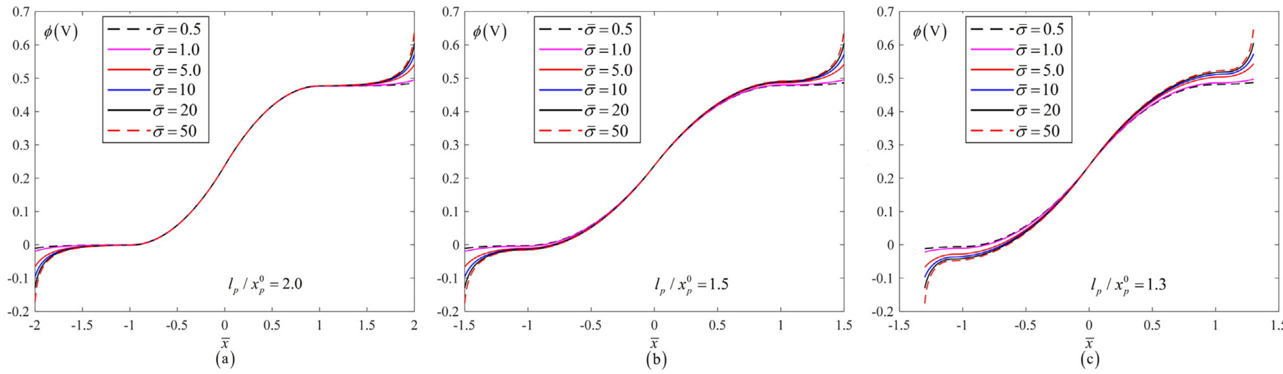

Fig. 3. Distribution of electric potential in a tensile-stressed piezoelectric PN junction for different $\bar{\sigma}$ with l_p/x_p^0 = 2.0, 1.5, 1.3, respectively.

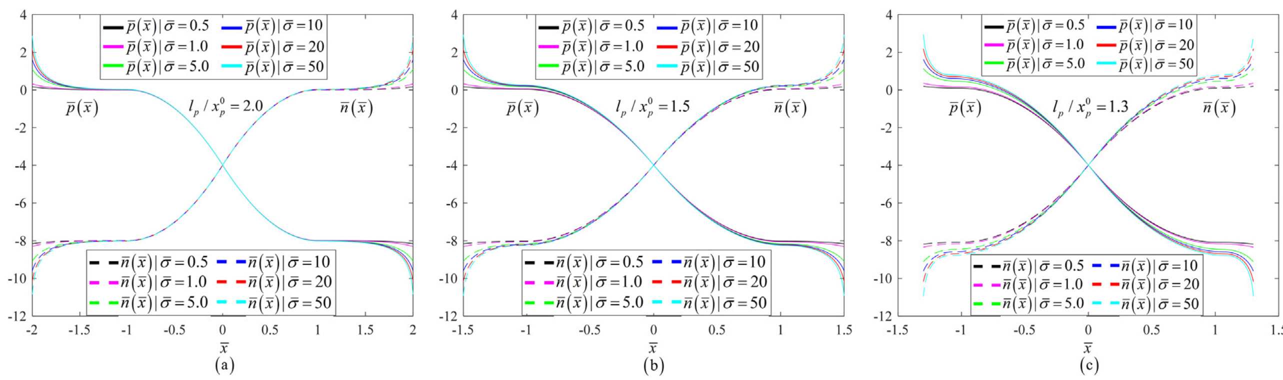

Fig. 4. Distribution of carrier concentrations in a tensile-stressed piezoelectric PN junction for different $\bar{\sigma}$ with l_p/x_p^0 = 2.0, 1.5, 1.3, respectively.

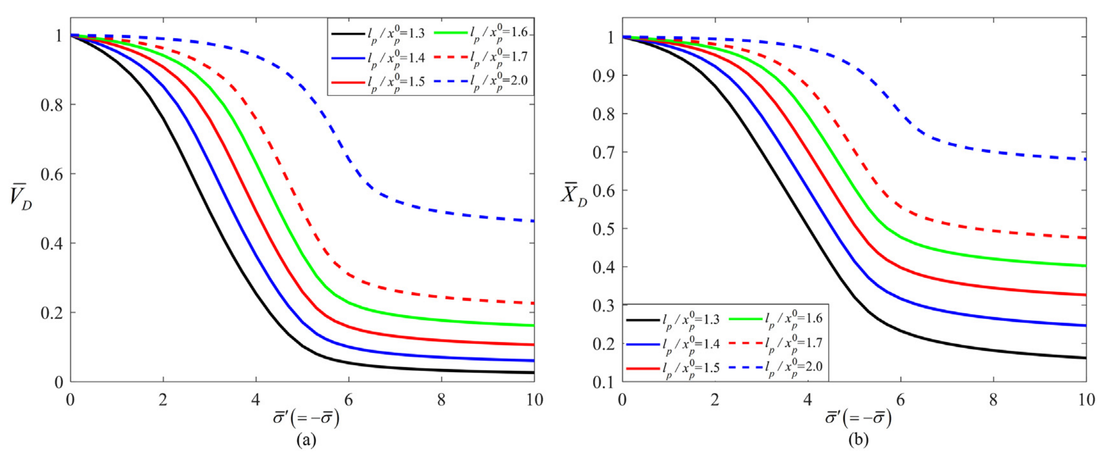

Fig. 5. Dependence of both the contact potential difference and the size of SCZ in a compressive-stressed piezoelectric PN junction for different l_p/x_p^0.

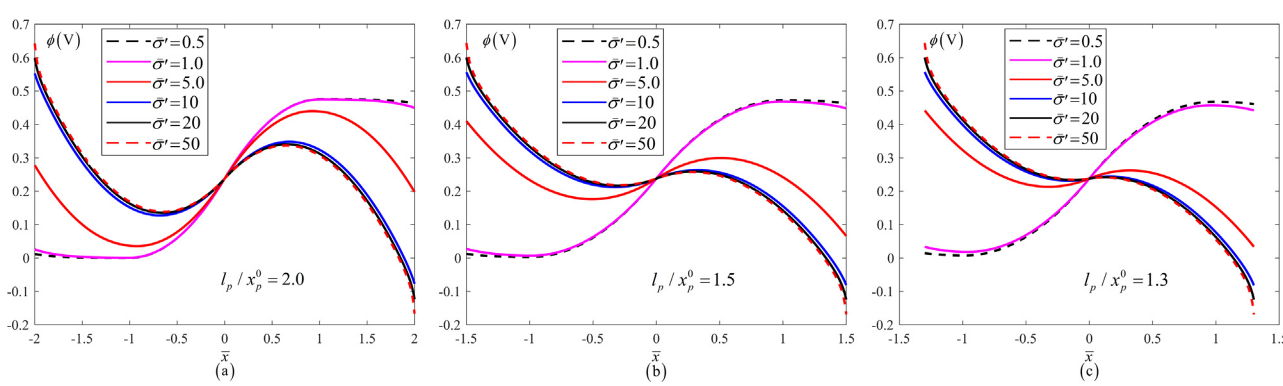

Fig. 6. Distribution of electric potential in a compressive-stressed piezoelectric PN junction for different $\bar{\sigma}'$ with l_p/x_p^0 = 2.0, 1.5, 1.3, respectively.

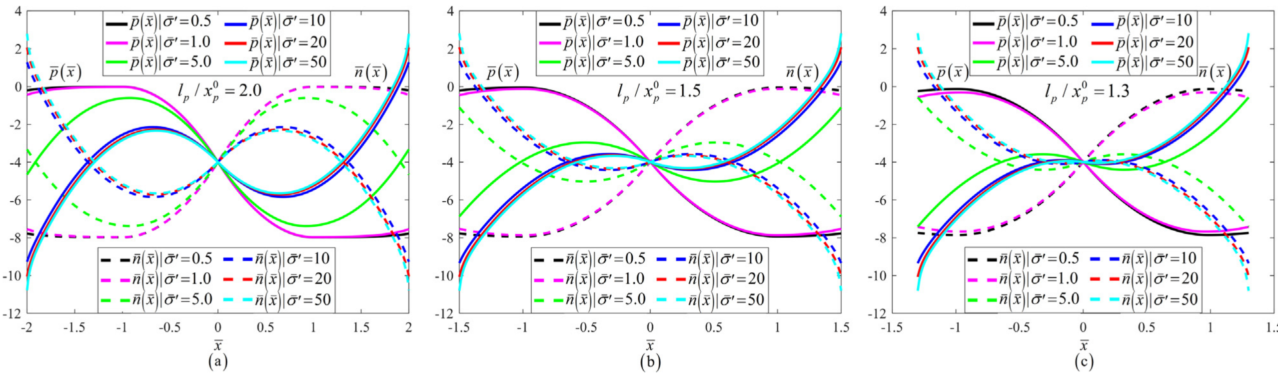

Fig. 7. Distribution of carrier concentrations in a compressive-stressed piezoelectric PN junction for different $\bar{\sigma}'$ with $l_p/x_p^0 = 2.0$, 1.5, 1.3, respectively.

increases in the p-type zone and that decreases in the n-type zone. According to the relationship between carrier concentrations and the Fermi energy level, we discover that the majority carrier concentration increases and the minority one decreases in both end regions of a tensile-stressed piezoelectric PN junction. These indicate that the contact potential difference of SCZ has been enlarged by tensile-stressed loading. In addition, when $l_p/x_p^0 = 2.0$ under $x_p^0 = 1.8285\mu m$, there exists a relatively large AR such that the electric potential increment stimulated by DIPEF has almost been cancelled by CRIEF. The upshot is that concentrations of majority carriers and minority carriers are almost unchanged at the SCZ boundary; When $l_p/x_p^0 = 1.5$, AR becomes small such that the influence from DIPEF has not yet been offset by CRIEF before arrived at SCZ. Therefore carrier concentrations appear slight fluctuation at $\bar{x} = \pm 1$. When $l_p/x_p^0 = 1.3$, AR becomes so small that serious influence from the coupled DIPEF and CRIEF certainly reaches SCZ. Under this situation, concentration of majority carriers becomes very great and concentration of minority carriers becomes very small at the SCZ boundary. Thus, a tensile-stressed piezoelectric PN junction with a smaller AR will become to possess greater electric potential difference, higher barrier and become more difficult to break-through.

Following, we pay attention to discuss the performance of a piezoelectric PN junction subjected to a pair of compressive-stresses $\bar{\sigma}'(=-\bar{\sigma})$. Fig. 5 shows dependence of $\overline{V}_D$ and $\overline{X}_D$ upon $\bar{\sigma}'$ for different l_p/x_p^0, where both quantities monotonously decrease with increasing compressive-stress. As known in the above, a smaller l_p/x_p^0 implies a shorter AR for CRIEF to produce weakening effect on DIPEF, and thus, is corresponding to larger variant rates of $\overline{V}_D$ and $\overline{X}_D$. Moreover, $\overline{V}_D$ and $\overline{X}_D$ appear two definite values finally after $\bar{\sigma}'$ increases to a certain degree, where the augmentation effect produced by mechanical-loading is just counteracted by the reduction effect caused by carrier redistribution.

When a ZnO rod with c-axis in the x-direction is subjected to a pair of compressive stresses at the two endpoints where electric displacement is null, the induced electric field in the rod is positive. Moreover, the electric potential is positive in the left portion and negative in the right one [33]. This indicates that in the PN junction in Fig. 1, the electric potential increment should be positive in the left p-zone and negative in the right n-zone. Fig. 6 shows distribution of electric potential field in a piezoelectric PN junction subjected to a pair of compressive-stresses, totally different from the situation for a tensile-stressed PN junction. Under compressive-stressed loading, both the contact potential difference and the size of SCZ are reduced with increase in $\bar{\sigma}'$. Similarly, interaction between the loading at $\bar{x} = -l_p/x_p^0$ and SCZ is very weak for $l_p/x_p^0 = 2.0$ such that the end loading produces very tiny influence on SCZ. When l_p/x_p^0 gradually becomes smaller, larger electric potential increment is stimulated in the SCZ boundary, for example $l_p/x_p^0 = 1.5$ and 1.3, and the contact potential difference will be decreased. As regards of carrier concentrations, they can be analyzed as follows: under compressive-stressed loading, the electric potential increment in the p-type zone is $\phi(x) > 0$ and the electric potential increment in the n-type zone is $\phi(x) - V_D^0 < 0$[33]. Thus, the intrinsic energy level of an electron in the p-type zone decreases and that in the n-type zone increases, which indicates that the majority carrier concentration decreases and the minority one increases in both end zones outside of SCZ. Of course, we also note that the magnitudes of incremental carrier concentrations are closely related to AR. When $l_p/x_p^0 = 2.0$ under $x_p^0 = 1.8285\mu m$, there exists a relatively large AR such that the electric potential increment caused by DIPEF has almost been cancelled by CRIEF before arrived at SCZ. The upshot is that concentrations of majority carriers and minority carriers are almost unchanged at the SCZ boundary; When $l_p/x_p^0 = 1.5$, AR becomes small such that the influence from DIPEF on SCZ has not yet been offset by CRIEF before arrived. Therefore carrier concentrations appear slight fluctuation at $\bar{x} = \pm 1$. When $l_p/x_p^0 = 1.3$, AR becomes so small that serious influence from the coupled DIPEF and CRIEF certainly reaches SCZ. It is readily found from Fig. 7 that concentration of majority carriers becomes very small and concentration of minority carriers becomes very great at the SCZ boundary. Obviously, a compressive-stressed piezoelectric PN junction with a smaller AR will become to possess smaller contact potential difference, lower barrier and becomes easier to break-through.

4. Conclusions

Explicit dependence of SCZ size, SCZ electric potential difference and carrier concentrations on external mechanical-loading has been obtained for a piezoelectric PN junction. In a tensile-stressed piezoelectric PN junction, the concentration of majority carriers goes up and the one of minority carriers cuts down such that the junction possess higher barrier and becomes more difficult to break-through; On the other hand, in a compressive-stressed piezoelectric PN junction, the concentration of majority carriers reduces and the one of minority carriers rises such that the junction is with lower barrier and becomes easier to break-through. The obtained results are useful in design of piezotronics and piezo-phototropic devices and the corresponding applications.

Acknowledgments

This work was supported by the National Natural Science Foundation of China [Grant Nos. 11672113 and 51435006] and the Key Laboratory Project of Hubei Province, China [No. 2016CFA073].

References

[1] A. Hutson, D.L. White, J. Appl. Phys. 33 (1962) 40–47.
[2] D.L. White, J. Appl. Phys. 33 (1962) 2547–2554.
[3] J. Collins, K. Lakin, C. Quate, H. Shaw, Appl. Phys. Lett. 13 (1968) 314–316.
[4] Y. Qin, X.D. Wang, Z.L. Wang, Nature 451 (2008) 809–813.
[5] R.S. Yang, Y. Qin, L.M. Dai, Z.L. Wang, Nat. Nanotechnol. 4 (2009) 34–39.
[6] S. Xu, Y. Qin, C. Xu, Y.G. Wei, R.S. Yang, Z.L. Wang, Nat. Nanotechnol. 5 (2010)

366–373.
[7] G. Zhu, R.S. Yang, S.H. Wang, Z.L. Wang, Nano Lett. 10 (2010) 3151–3155.
[8] Z.L. Wang, Adv. Funct. Mater. 18 (2008) 3553–3567.
[9] Z.L. Wang, R.S. Yang, J. Zhou, Y. Qin, C. Xu, Y. Hu, Y.F. Hu, S. Xu, Mater. Sci. Eng. R Rep. 70 (2010) 320–329.
[10] C.H. Wang, W.S. Liao, N.J. Ku, Y.C. Li, Y.C. Chen, L.W. Tu, C.P. Liu, Small 10 (2014) 4718–4725.
[11] R.S. Dahiya, G. Metta, M. Valle, A. Adami, L. Lorenzelli, Appl. Phys. Lett. 95 (2009) (034105-1-3).
[12] Z.F. Zhao, Xiong Pu, C.B. Han, C.H. Du, L.X. Li, C.Y. Jiang, W.G. Hu, Z.L. Wang, ACS Nano 9 (2015) 8578–8583.
[13] Y.R. Wu, J. Singh, Appl. Phys. Lett. 85 (2004) 1223–1225.
[14] W.Z. Wu, C.F. Pan, Y. Zhang, X.N. Wen, Z.L. Wang, Nano Today 8 (201) 619-642.
[15] W. Liu, A.H. Zhang, Y. Zhang, Z.L. Wang, Nano Energy 14 (2015) 355–363.
[16] Y. Zhang, Y. Liu, Z.L. Wang, Adv. Mater. 23 (2011) 3004–3013.
[17] Z.L. Wang, Mater. Sci. Eng. R Rep. 64 (2009) 33–71.
[18] P.A. Mante, Y.R. Huang, S.C. Yang, T.M. Liu, A.A. Maznev, J.K. Sheu, C.K. Sun, Ultrasonics 56 (2015) 52–65.
[19] S. Büyükköse, A. Hernandez-Minguez, B. Vratzov, C. Somaschini, L. Geelhaar, H. Riechert, W.G. van der Wie, P.V. Santos, Nanotechnology 25 (2014) (135204-1-6).
[20] Z.L. Wang, Adv. Mater. 15 (2003) 432–436.
[21] J. Yu, S.J. Ippolito, W. Wlodarski, M. Strano, K. Kalantar-Zadeh, Nanotechnology 21 (2010) (265502-1-8).
[22] K.Y. Lee, B. Kumar, J.S. Seo, K.H. Kim, J.I. Sohn, S.N. Cha, D. Choi, Z.L. Wang, S.W. Kim, Nano Lett. 12 (2012) 1959–1964.
[23] K.Y. Lee, J. Bae, S.M. Kim, J.H. Lee, G.C. Yoon, M.K. Gupta, S.J. Kim, H. Kim, J.J. Park, S.W. Kim, Nano Energy 8 (2014) 165–173.
[24] S.Y. Chung, S. Kim, J.H. Lee, K. Kim, S.W. Kim, C.Y. Kang, S.J. Yoon, Y.S. Kim, Adv. Mater. 24 (2012) 6022–6027.
[25] Y.X. Luo, R.R. Cheng, C.L. Zhang, W.Q. Chen, J.S. Yang, Acta Mech. Solid. Sin. 31 (2018) 127–140.
[26] K. Huang, R.Q. Han, The Physical Basis Of Semiconductors, The Science Publishing Company, Beijing, 2015.
[27] Z.L. Wang, Piezotronics and Piezo-phototronics, The Science Publishing Company, Beijing, 2014.
[28] S.Q. Fan, Y.X. Liang, J.M. Xie, Y.T. Hu, Nano Energy 40 (2017) 82–87.
[29] Y.X. Liang, S.Q. Fan, X.D. Chen, Y.T. Hu, Beilstein J. Nanotechnol. 9 (2018) 1917–1925.
[30] J.S. Yang, Acta Mech. Solid. Sin. 30 (2017) 21–26.
[31] Y.F. Gao, Z.L. Wang, Nano Lett. 7 (2007) 2499–2505.
[32] Y.T. Hu, Y. Zeng, J.S. Yang, Int. J. Solids Struct. 44 (2007) 3928–3938.
[33] C.L. Zhang, X.Y. Wang, W.Q. Chen, J.S. Yang, Smart Mater. Struct. 26 (2017) (025030-1-8).

Shuaiqi Fan is a Ph.D. candidate in Department of Mechanics at Huazhong University of Science and Technology, Wuhan, China. His research interests mainly focus on piezoelectric semiconductor structures and devices.

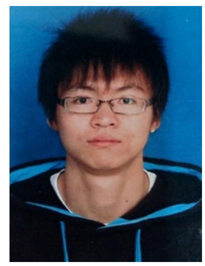

Wanli Yang is a Ph.D. Candidate in Department of Mechanics, Huazhong University of Science and Technology. Research interests are on micro/nano composite structures and piezoelectric semiconductor devices.

Yuantai Hu received his B.S. degree in 1986 from Wuhan University of Science and Technology, Wuhan, China, and his M.S. and Ph.D. degrees in mechanics, respectively, from Harbin University of Technology, Harbin, China, in 1988, and from the Shanghai Institute of Applied Mathematics and Mechanics, Shanghai University, Shanghai, China, in 1992. His research area is piezoelectric structures and devices, piezoelectric semiconductor structures, ultrasonics, and acoustics.